Applied Catalysis B: Environmental 300 (2022) 120747

Contents lists available at ScienceDirect

Applied Catalysis B: Environmental

journal homepage: www.elsevier.com/locate/apcatb

How substituent effects influence the thermodynamics and kinetics of gas-phase transesterification of alkyl lactates to lactide using TiO_2/SiO_2

Guillaume Pomalaza [a,1], Rik De Clercq [b,1], Michiel Dusselier [a,*], Bert Sels [a,*]

[a] Center for Sustainable Catalyis and Engineering KU Leuven Celestijnenlaan 200 F, 3001 Heverlee, Belgium
[b] Transfurans Chemicals, Leukaard 2, 2440 Geel, Belgium

ARTICLE INFO

Keywords:
Lactide
Alkyl lactate
Titanium-silica
Transesterification

ABSTRACT

Lactide, a crucial precursor of the bioplastic polylactic acid, was obtained through the gas-phase transesterification of alkyl lactates using a 5 wt% TiO_2/SiO_2 catalyst as an alternative to the conventional liquid-phase process. Lactide selectivity above 80% was achieved at 220 °C but conversion was thermodynamically limited at around 50% for all alkyl lactates. The nature of the ester alkyl chain had minimal impact of the thermodynamics of the reaction, but significantly influenced its kinetics. The Taft equation indicated that this kinetic effect was due to the polarity of the alkyl chain. Mechanistic studies indicated that lactide formed via a Langmuir-Hinshelwood mechanism involving two lactate molecules. The derived kinetic expression was fitted to experimental data of methyl lactate transesterification, resulting in a reduced chi-squared of 0.99 and an activation energy of 89.8 $kJ \cdot mol^{-1}$. Initial rate kinetics confirmed that the proposed mechanism was valid for other alkyl lactate species.

1. Introduction

Synthetic polymers are omnipresent in the products we use in of our daily lives. Unfortunately, conventional plastics have a detrimental impact on our environment throughout their life cycle. Plastics are primarily produced from non-renewable fossil resources through energy-intensive processes that emit large quantities of greenhouse gases [1]. Furthermore, because of their longevity, plastic wastes have accumulated in many environments, causing harm to local life [2]. Maintaining and improving our current standards of living without further damaging the environment requires that plastic manufacturing and disposal become sustainable.

Bioplastics—plastics produced from biomass or by living organisms—can alleviate some of the issues caused by conventional plastics as they are not derived from petroleum and are often biodegradable [3]. However, despite their advantages, bioplastics only account for less than one percent of global plastic production [4].

Part of the issue can be attributed to the poor competitivity of biorefineries versus their fossil-based counterparts [5]. First, because crude oil is inexpensive. Second, because the complex structure and properties of biomass result in higher processing costs [6]. To overcome these issues and make bioplastics a feasible alternative to plastics requires new and improved technologies.

One promising bioplastic which has attracted significant attention since the 1990s is polylactic acid [7]. Relatively biodegradable [8], compostable and produced from biosourced lactic acid, it is used primarily in the packaging and textile industries where it is able to compete with petroleum-based plastics. With 200,000 tons produced yearly, polylactic acid represents a global market worth USD 535.5 million in 2019 which is expected to grow by 16% yearly for the next 7 years [9]. Nevertheless, polylactic acid manufacturing is not without its problems.

High-quality polylactic acid is currently obtained via the ring-opening polymerization of lactide (LD), the cyclic dimer of lactic acid [10]. LD itself is produced from the depolymerization of low-quality polylactic acid synthesized from lactic acid by polycondensation. However, not only is this multistep process energy intensive, but the racemization that occurs during depolymerization results in a less enantiomerically pure polymer, which affects its quality and reducs its range of applications. These limitations are being tackled with by the scientific community through new pathways leading to LD [7,11–15].

Catalytic gas-phase reactions in fixed bed reactors are a promising alternative due to their improved performances. By directly converting

* Corresponding authors.
E-mail addresses: michiel.dusselier@kuleuven.be (M. Dusselier), bert.sels@kuleuven.be (B. Sels).
[1] These authors contributed equally to this work as co-first authors.

https://doi.org/10.1016/j.apcatb.2021.120747
Received 7 June 2021; Received in revised form 3 September 2021; Accepted 21 September 2021
Available online 25 September 2021

lactic acid to LD, these processes omit the costs associated with conventional LD production which takes two steps—oligomerization and depolymerization—and requires near-vacuum conditions. In addition, gas-phase reactions have shown to be highly enantiomerically selective and highly productive despite shorter residence time [10]. Furthermore, the use of heterogeneous catalysis, compared to the conventional LD production method, simplifies the recycling of both feedstock and catalyst, which generally consists of bulk or supported metal oxides [11,16,17]. However, there are some limitations associated with these gas-phase processes, primarily due to the unavoidable water content in commercial lactic acid feedstock in liquid form. Because of the high vaporization enthalpy of water, aqueous lactic requires more energy to be vaporized. Furthermore, even moderately concentrated aqueous lactic acid contains lactic oligomers which cause practical issues due to their increased weight. In addition, water lowers the space-time yield of the process and exposes LD to degradation via hydrolysis during storage [18]. Finally, lactic acid is highly diluted in the carrier gas [17], i.e. 1.5 mol% in N_2 as per Park et al. [12], further reducing the space-time yield of these processes [10].

We previously proposed a novel one-step gas-phase process to produce LD that deals many of the problems identified above by instead using (L)-methyl lactate—an ester of lactic acid—as feedstock [19,20]. Using silicate-supported TiO_2 catalysts, (L)-methyl lactate (hereinafter abbreviated to MLA) has been be converted to LD with minimal byproduct formation at temperatures ranging between 220 and 260 °C. LD is formed from two MLA molecules via a double transesterification, which is the process of exchanging the alkoxy group of an ester with an alcohol, thereby generating another ester and alcohol. A thorough characterization of our catalyst has revealed that highly dispersed TiO_2 nanoparticles were the active sites for this transesterification [20].

Prepared through the esterification of lactic acid with methanol [21], and a byproduct of lactic acid purification, or alternatively through direct conversion of sugars [22] or propylene glycol [23], MLA is currently sold as a biodegradable solvent [24,25]. Using it to produce value-added LD is of high interest to the polylactic acid industry, notably because it retains the advantages of gas-phase processes, while addressing some of the issues associated with aqueous lactic acid-based processes, such as the use of a water-free feedstock and the ability to work in concentrations up to 25% in N_2 [12,20].

However, MLA is not the only interesting feedstock for our catalytic process: other alkyl lactates such as ethyl lactate (ELA) and n-butyl lactate (BLA)—also obtained as byproducts of lactic acid purification [25]—also have the potential to form LD via transesterification (Scheme 1). Using alkyl lactates other than MLA avoids toxic methanol in either the lactate synthesis or as the byproduct of LD production [26,27]. Indeed, our technology has already demonstrated that it can be applied for the cyclization of other α-hydroxy esters, namely glycolate, providing new routes to other bioplastics [28]. Therefore, the aim of this work is to expand the pool of alkyl lactates suitable for producing LD using our catalytic system—in this case 5 wt% TiO_2/SiO_2.

We investigated the effect of the alcohol leaving group on the transesterification to L-lactide (L-LD) by using methyl, ethyl, isopropyl and n-butyl lactate. Although these compounds all possess the required lactate backbone to form LD, the importance of their leaving group on transesterification performances had yet to be evaluated. By providing new insight into the equilibrium, kinetics, and mechanism of the transesterification of alkyl lactate to L-LD, this work broadens the applicability of our TiO_2/SiO_2 catalyzed process, opening new possibilities for producing bioplastics.

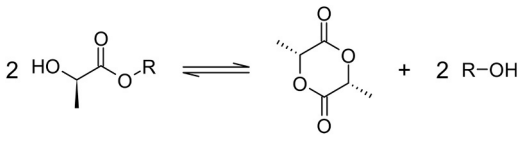

Scheme 1. Alkyl lactate transesterification reaction.

2. Experimental

2.1. Materials

A silica-supported TiO_2 catalysts with 5 wt% of metal oxide was prepared through the incipient wetness impregnation of an amorphous, large-pore SiO_2 gel (Alfa Aesar, 287 $m^2 \cdot g^{-1}$, pore volume of 0.91 $cm^3 \cdot g^{-1}$) using a suitable amount of titanium isopropoxide dissolved in 2-propanol, as described in our earlier work [19,20]. After impregnation, the solid was dried in an oven at 80 °C then calcined at 500 °C in static air for 4 h with a heating rate of 5 °C per minute. Characterization of said material can be found in these publications.

(L)-Methyl lactate (>97%) was purchased from Acros Organics. (L)-Ethyl lactate (>98%) and (L)-Butyl lactate (>98%) were purchased from Sigma Aldrich. (L)-Isopropyl lactate (>98%) was kindly provided by Galactic (Galaster IPL 98). Chemicals were used without further purification.

2.2. Catalytic reactions

Catalytic reactions with the various alkyl lactates were performed in a custom-built fixed-bed high-throughput reactor consisting of 6 parallel independent quartz reactors (length 480 mm, inner diameter of 4 mm). Typically, 10 – 300 mg of catalysts sieved to 250 – 500 μm were inserted in the reactors and held in place by quartz wool. Inert quartz pellets (125 – 250 μm) were used to dilute the catalyst and to achieve a minimum bed weight of 300 mg. Catalysts were pretreated at 300 °C under a 20 $ML \cdot min^{-1}$ nitrogen flow for at least an hour before each reaction and left to cool down to the desired reaction temperature. Feed solutions consisted of 95 vol% alky lactate mixed with 5 vol% ortho-xylene (99%, Acros organics) as internal standard. Using a Waters 515 HPLC pump, the reaction feed was evaporated at 210 °C and mixed with a nitrogen flow—typically 20 $ML \cdot min^{-1}$—and introduced into the reactors. The output of each reactor was diluted with an additional 30 $ML \cdot min^{-1}$ nitrogen flow and analyzed with an on-line GC. For each data point recorded, several injections were made over a period of two hours on average, and the average value was recorded. Deactivation was negligeable over multiple hours on stream under different reaction conditions.

2.3. Analysis

Effluent gases were analyzed with an on-line GC (HP 6890 series) equipped with an Agilent CP-Sil 24 CB capillary column and a Flame ionizing Detector. Catalytic performances were measured according to the following metrics:

$$Conversion(\%) = \frac{moles\ of\ ester\ fed - moles\ of\ ester\ remaining}{moles\ of\ ester\ fed}$$

$$Selectivity(\%) = \frac{moles of product formed \cdot moles of ester incorporated in the product}{moles of ester converted}$$

$$Yield(\%) = Conversion \cdot Selectivity$$

$$\frac{W}{F_0} = \frac{catalyst\ mass \cdot hour}{moles\ of\ ester\ fed}$$

2.3.1. Methyl lactate transesterification kinetic study

Using the same high-throughput reactor, the exit flow of every reactant was measured at different reaction temperatures, initial MLA partial pressures and contact times for a total of 30 independent data points. Temperatures were 220, 240 and 260 °C, with initial MLA partial pressures of 2.4, 5.9, 9.3. 15.3 and 25.7 kPa and $W/F_{MLA}{}^0$ between 0.7

and 24.7 $g_{cat}{\cdot}h{\cdot}mol_{MLA}^{-1}$.

$$\frac{dF_i}{dW} = r_i \tag{1}$$

The rate of formation of compound i was represented by Eq. (1) where F_i is the exit molar flow rate for compound i ($mmol{\cdot}h^{-1}$) and W the mass of catalyst (g). In all cases, the ratios of particle diameter to reactor diameter and particle diameter to bed length were large enough to ensure plug flow conditions [29]. Because conversion was generally above 10%, integral reactor conditions were considered when interpreting the experimental data. Furthermore, we assumed that the catalyst operated under steady-state conditions and that a single type of active site was homogeneously dispersed on its surface—for more information on the structure-activity relationship of silicate-supported TiO_2 catalysts, we invite the reader to consult our previous publications [19,20]. Interparticle diffusional limitations were excluded as demonstrated by precedent work [20].

The models elaborated as part of this kinetic study (see Section 3.3.2.) were converted to rate expressions, introduced into Eq. (1) and solved numerically using the *odeint* function of the SciPy library [30]. Kinetic parameter estimation was done using the *minimize* function of the *lmfit* package [31] which performs a non-linear least-square fit of the reactant exit flow derived from our rate expressions with the experimental data. The *lmfit* package also provided useful fit statistic through the *fit_report* function, such as the reduced chi-squared (χ_v^2) statistic, the Bayesian Information Criterion (BIC) and confidence intervals of the estimated parameters. Rate expressions were reparametrized using a reference temperature optimized according to the procedure detailed by Schwaab and Pinto to simplify the fitting procedure [32].

The dependence of the kinetic parameters on temperature was expressed as an Arrhenius law for the kinetic constants for reaction number n (k_n) and as a Van't Hoff law for the adsorption constants of compound i (K_i), as indicated in Eqs. (2) and (3), respectively.

$$k_n = k_{0,n}{\cdot}exp\left(\frac{-E_{a,n}}{R{\cdot}T}\right) \tag{2}$$

$$K_i = K_{0,i}{\cdot}exp\left(\frac{-\Delta H_i}{R{\cdot}T}\right) \tag{3}$$

where $k_{0,n}$ and $K_{0,i}$ are the preexponential factors, $E_{a,n}$ is the activation energy of reaction n and ΔH_i is the enthalpy of adsorption of component i.

3. Results & discussion

3.1. Alkyl chain influence on transesterification thermodynamics

In our previous papers [19,20], we demonstrated that MLA transesterification on 5 wt% TiO_2/SiO_2 was thermodynamically limited: at 220 °C with an initial lactate partial pressure of 5.8 kPa, conversion plateaued around 50%. Conversion could be increased by raising the reaction temperature, but selectivity towards the desired cyclic dimer dropped significantly because undesired side-reactions, such as decarbonylation to acetaldehyde, started to occur, restricting the operating conditions of the process.

In the present study, a comparable conversion threshold of 47.5 ± 3.0% was observed regardless of the type of alkyl lactate used. Likewise, at equivalent conversion rates, selectivity towards LD was comparable for all alkyl lactate tested, averaging 84.2 ± 6.8% (Fig. 1).

As illustrated in Fig. 2, the nature of the substrate did not drastically change the product distribution at equilibrium. Independently of the alkyl lactate reacted, similar distributions of LDs, linear dimers and other byproducts were obtained when transesterification was conducted under equilibrium conditions at the same temperature and comparable initial partial pressure.

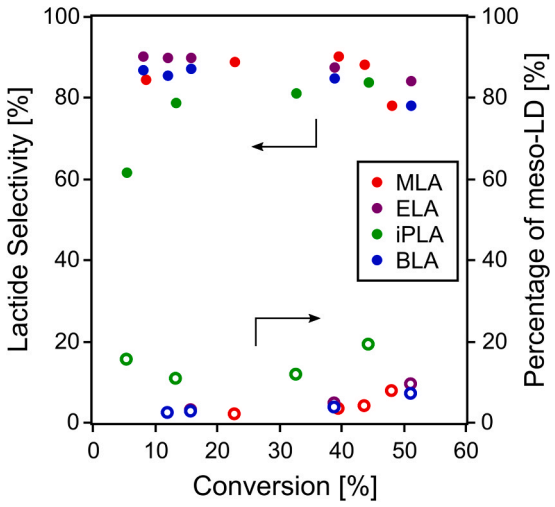

Fig. 1. Selectivity toward LD (closed symbols), percentage of meso-LD (open symbols) as a function of alkyl lactate conversion. Conditions: 220 °C, $W/F_{lactate}$ = 4 – 120 $g_{cat}{\cdot}h{\cdot}mol^{-1}$. Lactate volume %: MLA, ELA, iPLA and BLA are 5.7%, 4.6%, 5.7% and 5.1% respectively.

In addition, Fig. 2 shows how catalytic performances at equilibrium varied in a similar manner under the effect of initial ester partial pressure. At low partial pressure, conversion and LD selectivity were the highest; increasing the partial pressure decreased the equilibrium conversion and promoted the selectivity towards linear dimers at the expense of LD. The similar product distribution observed at equilibrium suggest that the different leaving groups have a limited effect on the thermodynamics of alkyl lactate transesterification.

One explanation for these observations is that the change in the free energy of formation varies similarly for each pair of alkyl lactate and corresponding alcohol as their alkyl chain gets longer. Accordingly, although the thermodynamic properties of each group is influenced by the alkyl chain lengths, their differences cancel each other out resulting in comparable changes in the free energy of the transesterification reaction. Because the free energy difference between the two sides of a reaction determines its extent, comparable free energy changes would result in comparable equilibrium. To investigate the merit of this explanation, we turned to the change in Gibbs free energy of formation.

As mentioned in our previous work, the thermodynamic properties of alkyl lactates available in the literature or in commercial databanks are inaccurate [19]. Therefore, we used the Gani group-contribution method to estimate the standard Gibbs free energy of formation of all organic compounds under study (Table S1) [33]. Although high accuracy of these values with this approach is not claimed, we believe it is sufficient to capture trends resulting from the growing alkyl chain of alkyl lactates and their corresponding alcohols. As can be seen in Figure S1, the changes in Gibbs free energy of reaction for all four transesterification reactions are very similar, highlighting the limited impact of the alkyl chain on transesterification thermodynamics.

Consequently, a process designed to operate at equilibrium is expected to perform equally well in terms of yield and selectivity regardless the nature of the alkyl chain of the ester function of the alkyl lactate pool.

3.2. Alkyl chain Influence on transesterification kinetics

The kinetics of alkyl lactate transesterification on 5 wt% TiO_2/SiO_2 were found to be influenced by the nature of their alkyl chain and the corresponding alcohol leaving group. As illustrated in Fig. 3, the apparent initial reaction rate, e.g. the tangent of conversion-space time curves at initial conversion [34], was highest for MLA, followed by ELA and BLA, and lastly by isopropyl lactate (iPLA). The difference between

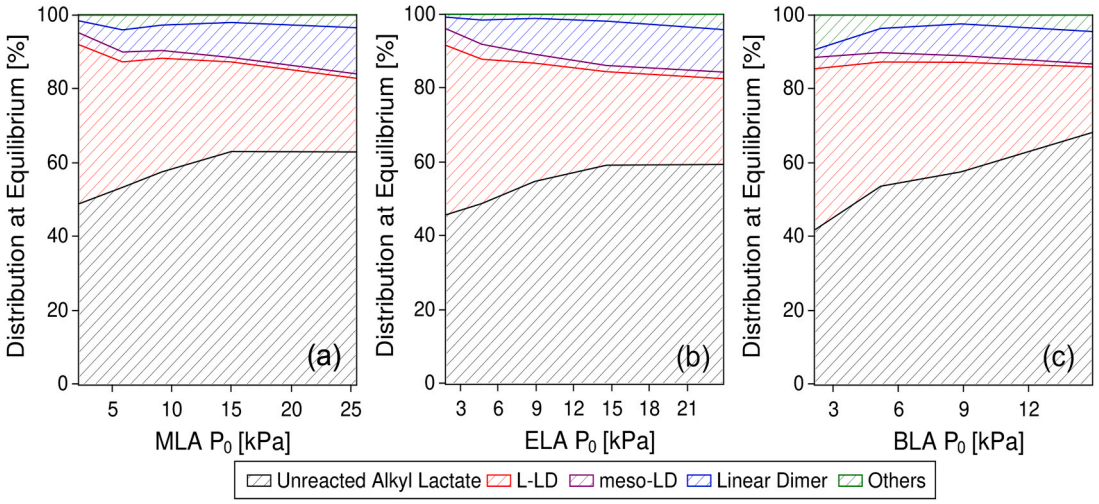

Fig. 2. Product distribution of lactate species at equilibrium for transesterification of: (a) MLA, (b) ELA and (c) BLA to LD with 5 wt% TiO_2/SiO_2 at different alkyl lactate concentration in N_2 (total pressure of 101.3 kPa). Reaction conditions: 220 °C, $W/F_0 > 39$ $g_{cat}{\cdot}h{\cdot}mol_{ester}^{-1}$.

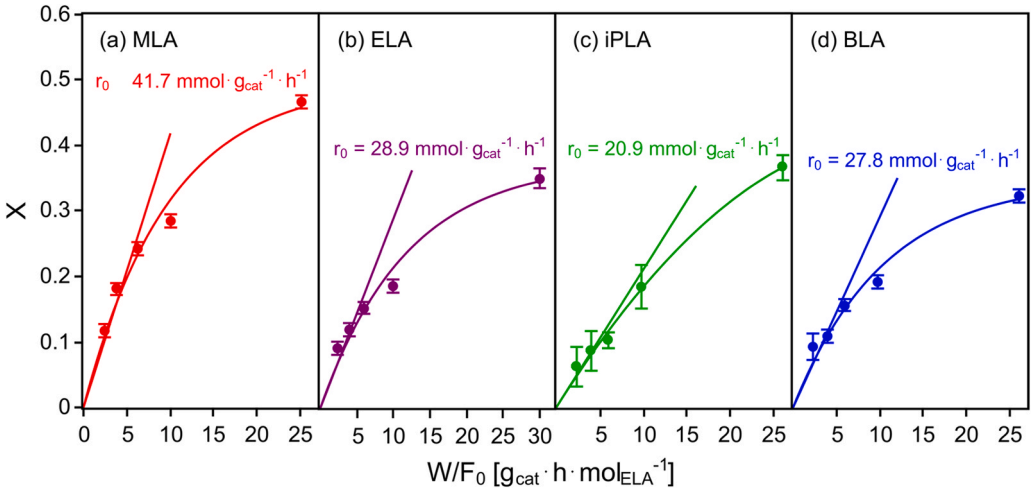

Fig. 3. Conversion curves and initial rates for alkyl lactate transesterification on 5 wt% TiO_2/SiO_2 as a function of contact time at 220 °C, partial pressure: 1.9 – 25.5 kPa of alkyl lactate. Straight lines represents the tangent at initial conversion of conversion curves (nonlinear fit).

the latter two suggests that transesterification occurs faster when the leaving group is a primary alcohol rather than a secondary alcohol.

The chain length of alkyl lactates with primary alcohol leaving group also appeared to affect the reaction kinetics as the reaction rate dropped sharply between MLA and ELA. However, considering the small difference in rate between ethyl and BLA, this effect does not follow a linear relationship with regards to the alkyl chain length. Fig. 4.

The kinetic effect observed was better explained by the different basic strengths of the alcohol leaving group produced during transesterification. As demonstrated in Fig. 5, apparent initial reaction rates of alkyl lactate were negatively correlated with the pKa values in water of their corresponding alcohol leaving groups; weaker bases are generally better leaving groups during nucleophilic substitution reactions [35].

The Taft equation Eq. (4) was used to further investigate the influence of the alkyl chain on the kinetics of alkyl ester transesterification on 5 wt% TiO_2/SiO_2. The Taft equation is a linear Gibbs energy relationship used to evaluate the polar and steric effects that a substituent, a minor part of a molecule which does not change the overall character of a reaction, may have on the kinetics and mechanism of a reaction [36,37]. This is achieved by solving Eq.4 with experimental kinetic constants, and using the values of the estimated parameters for mechanistic interpretation.

$$log(k_{rel}) = \rho^{*}{\cdot}\sigma^{*} + \delta^{*}{\cdot}E_s \quad (4)$$

These parameters are ρ* and δ, respectively the polar and steric sensitivity factors, which represent how much steric and polar effects influence a given reaction. Eq. (4) also contains σ* and E_s, which are empirical constants that represent the contribution of substituents to the polar and steric effects; the constants of many substituents are available in the literature [38].

For our study of alkyl lactate transesterification, the substituents considered the alkyl chains of the ester group. The values for σ* and E_s, were retrieved from Datta [38]. Furthermore, the term k_{rel} was approximated as the initial reaction rate identified in Fig. 3 divided by the initial reaction of MLA transesterification.

Fig. 5 is the parity plot between experimental rates and the calculated rates at 220 °C determined with Eq. (4). As illustrated, the correlation yielded a good linear relationship, indicating that the reaction is adequately described by the fitted sensitivity factors. The ρ* and δ factors thus obtained were 1.47 and $3.01{\cdot}10^{-3}$, respectively. The low value of δ suggests that alkyl lactate transesterification is not affected by steric effects from the ester alkyl chain. Instead, it is the polar effects of these substituents that largely govern the reaction kinetics, as evidenced by

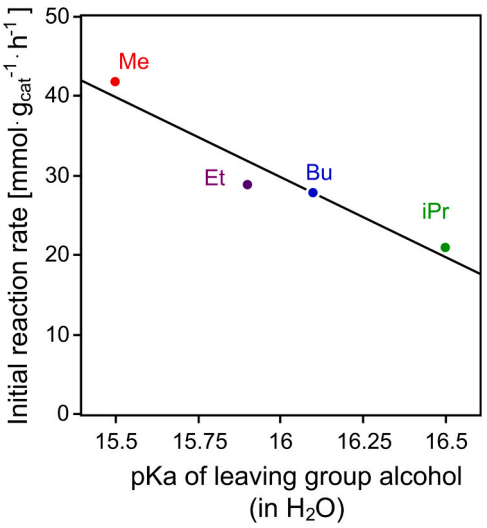

Fig. 4. Comparison of initial transesterification rate at 220 °C for different alkyl lactates and the pKa of their corresponding leaving group alcohol in water.

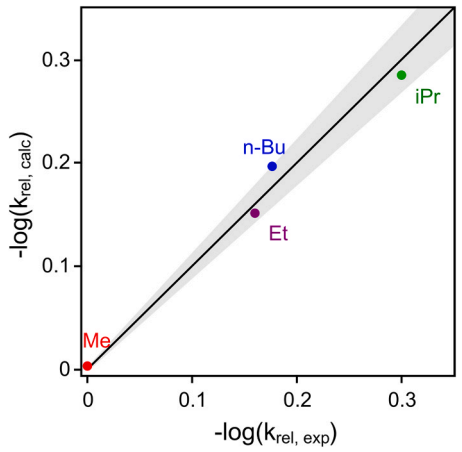

Fig. 5. Taft plot of transesterification of alkyl lactates at 220 °C; gray area represents a ± 10% deviation.

the comparatively greater ρ* factor. Its positive value further indicates that the transesterification is accelerated by electron withdrawing groups.

Due to their greater electron donating properties, we conclude that alkyl lactates with longer and/or more substituted alkyl groups will have lower transesterification rates. For instance, using the solved Taft equation (Eq. (4)) with the factors available in the literature [38], the initial transesterification rate of *tert*-butyl lactate with 5 wt% TiO_2/SiO_2 is predicted to be 14.7 mmol·g_{cat}^{-1}·h^{-1}, or about one third of the rate obtained with MLA. Consequently, the pool of alkyl lactates available to our gas-phases process is—economic considerations aside—limited by the electron donating properties of the alkyl ester chain, which could make transesterification kinetically impracticable beyond a certain point.

3.3. Alkyl lactate transesterification mechanism

3.3.1. Analytical study of the mechanism & pathway of MLA transesterification

As demonstrated above, the kinetics of alkyl lactate transesterification with 5 wt% TiO_2/SiO_2 are accurately described a Taft equation that considers the alkyl group of the ester as the substituent. Therefore, we can conclude that the rate-determining step of the reaction is the alcohol elimination step, which is the transesterification itself, as it predominantly involves this alkyl group. However, because the pathway to LD has not been elucidated, there are three potential transesterification steps that could be considered rate-determining. As shown in Scheme 1, alkyl lactates could be directly transesterified to LD, or could undergo a double transesterification, first to their linear dimer, then to LD (Scheme 2).

What position the linear dimers and LD occupy in the overall reaction pathway of alkyl lactate transesterification was studied by the delplot method using MLA as reference. Developed by Bhore et al. [39], this technique is used to deduce reaction networks by discerning primary and secondary products through visual interpretation of kinetic plots. Simply put, selectivity towards the products are plotted against conversion and extrapolated to the abscissa; the order by which the products appear is determined by the y-intercept, and their stability by the appearance of the fitted curve.

Fig. 6 depicts the delplot method applied to the results of MLA transesterification with 5 wt% TiO_2/SiO_2. As their extrapolated selectivity has a finite y-intercept, L-LD and methyl lactyl lactate (ML_2A) are considered primary products, meaning they are directly obtained from MLA. Contrarily, because the extrapolated selectivity of meso-LD tends to zero, it is regarded as a secondary product. Although the near zero slope of the fitted curves for ML_2A and L-LD suggests that these products are stable, the decrease in L-LD selectivity at high conversion also denotes that consumption of the latter takes place, ostensibly to form meso-LD through racemization at higher conversion. Therefore, delplot analysis of MLA transesterification indicates that the linear dimer is a primary stable product, L-LD is a primary unstable product, and meso-LD is a secondary product, possibly formed from the racemization of lactate species, although the identity of these intermediates has not yet been established. Visual inspection of Fig. 1 indicates that the same conclusion can be reached for the reaction pathway of transesterification using other alkyl lactates, except with iPLA for which the extrapolation of meso-LD suggests instead that it is a primary product.

To acquire further mechanistic understanding of alkyl lactate transesterification into cyclic and linear dimers, an initial rate study of LD and ML_2A formation from MLA on 5 wt% TiO_2/SiO_2 was conducted. Initial rate studies are practical tools for kinetic analysis: by considering reaction rates near zero conversion, the influence of product adsorption and reaction equilibria become negligible compared to the concentration of initial species, thereby simplifying rate law expressions. For simple reactions, the shape of the rate curves obtained by plotting initial rates against initial concentration—in this case partial pressure—can be correlated to plausible reaction mechanisms [40].

Fig. 7 shows the initial rates of transesterification to total LD (the sum of L-LD and meso-LD since the latter was negligible at low conversion) and ML_2A with regards to the initial partial pressure of MLA. As can be seen, the initial LD formation rate displayed a non-linear

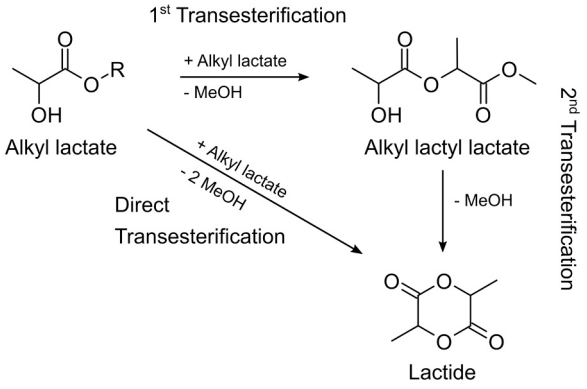

Scheme 2. Possible reaction pathways leading to LD from alkyl lactate.

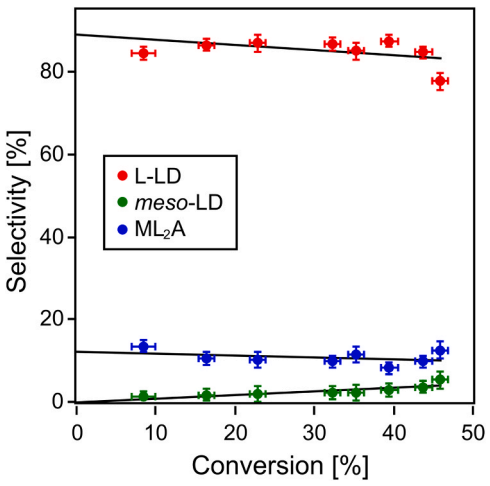

Fig. 6. Delplot analysis of MLA at 220 °C, initial partial pressure of 5.9 kPA, total pressure of 101.3 kPa and W/F_0 between 3 and 40 $g_{cat}{\cdot}h{\cdot}mol_{MLA}^{-1}$.

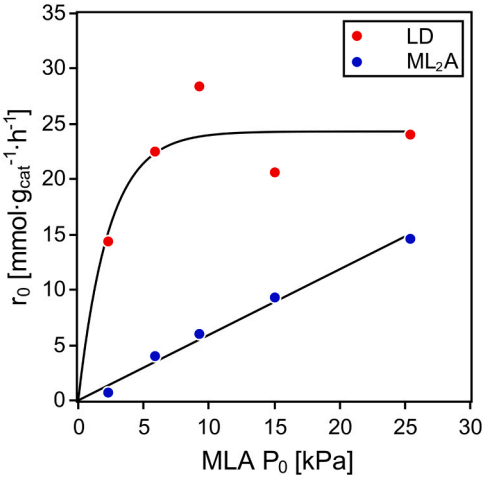

Fig. 7. Initial formation rate of LD and MLA as a function of initial partial pressure of MLA at 220 °C. Curves represent the best mathematical fit.

dependency on MLA partial pressure characterized by a plateau at higher pressure. Contrarily, initial ML_2A formation rate increased linearly with MLA partial pressure.

The non-linear plateauing shape of the LD formation curve is a strong indication that the transesterification rate is controlled by a dual-site surface reaction, that is to say a Langmuir-Hinshelwood type reaction mechanism [40,41].

The linear rate curve observed for ML_2A formation is generally associated with bimolecular reactions controlled by the adsorption of one reactant [42], but could also be attributed to a surface-controlled Eley-Rideal mechanism—the ambiguity lies in that an Eley-Rideal rate curve, although it begins as the square of the pressure, becomes directly proportional to the pressure as it increases [40]. Thus, the extrapolation to the origin of the linear fit, illustrated in Fig. 7, may be hiding a non-linear shape at partial pressure lower than 5 kPa. Whether or not this is the case, we can nevertheless conclude that the rate-limiting steps for the formation rate of each dimer follows different mechanisms.

3.3.2. Numerical study of the mechanism & pathway of MLA transesterification

With the insight acquired by the delplot analysis and initial rate study, we could narrow down the potential mechanism and pathway of MLA to LD and ML_2A. To assess their validity, Langmuir-Hinshelwood-Hougen-Watson (LHHW) rate laws were derived and compared to experimental data gathered at different MLA partial pressure, contact time, and temperatures ranging from 220° to 260°C.

In total, four models were elaborated (Table 1). The first two models sought to discriminate between the two possible mechanisms identified by the shapes of the rate curves in the initial rate study. In model 1 (Ads.-LH), ML_2A formation was determined by the rate of adsorption of MLA—as suggested by the linear curve observed in Fig. 7—whereas LD formation followed a Langmuir-Hinshelwood type mechanism, as per the non-linear shape of its respective rate curve. Model 2 (ER-LH) accounted for the alternative interpretation that the linear rate curve of ML_2A formation in Fig. 7 may instead indicate an Eley-Rideal type mechanism, which has been identified as the mechanism of liquid-phase transesterification reactions [43,44].

The last two models were not based on the results of our analytical mechanistic study but considered the possibility that it may have failed to capture all the mechanistic details of the reaction. Model 3 (LH-LH) thus considered that both dimers are formed through Langmuir-Hinshelwood type mechanisms with the surface reactions being rate determining, since Eley-Rideal type mechanisms are uncommon in gas phase catalytic reactions [45]. Model 4 (Consecutive) ran contrary to the results of our delplot analysis of the reaction pathway and theorized that ML_2A is an intermediate specie for the formation of LD, a possibility which was proposed in our previous papers; [19,20] it assumed an adsorption-determined rate for ML_2A formation and a dual-site mechanism for LD formation, as per the rate curves in Fig. 7.

To reduce the complexity of solving the kinetic equations, we employed several approximations and simplifications:

- The reactor was modelled as an integral reactor because conversion was above 10%.
- The catalyst was considered to operate under steady-state condition. Deactivation was negligeable over several hours on stream.
- Interparticle transfer limitations were excluded based on our previous work [20].
- Reaction rates were assumed to be governed by rate-determining elementary reaction steps with which all other steps are in quasi-equilibrium.
- Only the formation of ML_2A and LD—the csum of L-LD and meso-LD amounts—as well as methanol were considered because selectivity towards other products remained low (<5%) under the conditions used.
- Only the partial pressures of MLA—the inhibiting effect of which on LD formation can be observed in Fig. 7—and methanol—the most abundant byproduct—were taken in account in the coverage of free active sites θ_*, as per Eq 5.

$$\theta_* = \frac{1}{1 + K_{MLA}{\cdot}p_{MLA} + K_{MeOH}{\cdot}p_{MeOH}} \tag{5}$$

- Reaction reversibility expressed through an equilibrium constant was omitted because of the difficulties previously encountered in determining accurate values for the equilibrium constants of MLA transesterification by experimental and theoretical approaches [19,20]. To mitigate the effects of this omission, data points were recorded at conversions 10–20% points below the apparent thermodynamic equilibrium or maximum conversion for each specific temperatures.

These approximations are acceptable because the primary aim of this kinetic study was to capture the qualitative behavior of the reaction for mechanistic elucidation purposes rather than for making quantitative predictions.

To find the best possible candidate, rival models were discriminated using the following statistical tests: the reduced chi-squared (χ_ν^2) statistic

Table 1
Kinetic model, their rate determining steps for the formation of ML_2A and LD with the corresponding rate law expression, reduced chi-square and Bayesian Information Criterion of best fits with experimental results.

No.	Name	RDS			Rate	χ^2_v	BIC
1	Ads.-LH	MLA +*	→	MLA*	$r_1 = k_1 \cdot p_{MLA} \cdot \theta_*$	1.46	75.6
		2MLA*	→	LD* + MeOH*	$r_2 = k_2 \cdot K^2_{MLA} \cdot p^2_{MLA} \cdot \theta^2_*$		
2	ER-LH	MLA* + MLA	→	ML_2A* + MeOH	$r_1 = k_1 \cdot K_{MLA} \cdot p^2_{MLA} \cdot \theta_*$	0.99	29.9
		2MLA*	→	LD* + MeOH*	$r_2 = k_2 \cdot K^2_{MLA} \cdot p^2_{MLA} \cdot \theta^2_*$		
3	LH-LH	2MLA*	→	ML_2A* +MeOH*	$r_1 = k_1 \cdot K^2_{MLA} \cdot p^2_{MLA} \cdot \theta^2_*$	11.0	318.3
		2MLA*	→	LD* + MeOH*	$r_2 = k_2 \cdot K^2_{MLA} \cdot p^2_{MLA} \cdot \theta^2_*$		
4	Consecutive	MLA +*	→	ML_2A*	$r_1 = k_1 \cdot p_{MLA} \cdot \theta_*$	4.90	228.2
		ML_2A* + *	→	LD* + MeOH*	$r_2 = k_2 \cdot K_{ML_2A} \cdot p_{ML_2A} \cdot \theta^2_*$		

k: kinetic constant; p_i: partial pressure of compound i. K_i: the adsorption equilibrium constant of compound i.

is a measure of the goodness-of-fit for which the best fit is closest to 1, and the Bayesian Information Criterion (BIC), which is used to compare models—the model with the lowest BIC being considered the best. The results of these tests are listed in Table 1 alongside their respective models.

Statistical test results indicate that the ER-LH model is the best model of all four, followed by the Ads.-LH model. With χ^2_v values close to one, both can be said to fit the experimental data adequately. However, the smaller BIC of the ER-LH model confirms its superior fit in that it minimizes the information lost between the calculated and experimental values. The quality of the ER-LH model is further illustrated by Fig. 8(a) and (b), which are parity plots comparing the measured vs. calculated conversion rates and compound flow out of the reactor, respectively. The distributions of data points along the diagonal line in both cases demonstrate that the ER-LH model correctly describes the data. Contrarily, the comparatively high χ^2_v and BIC values suggest that the other two models—the LH-LH and Consecutive models—poorly describe the experimental data, confirming that the analytical studies of transesterification had correctly captured the essential mechanistic information of the reaction.

The kinetic parameters estimated from the fitting of model ER-LH are summarized in Table 2. As listed, the 46.7 kJ·mol^{-1} activation energy of ML_2A formation (linear dimer, $E_{a,1}$) is significantly lower than that of LD (cyclic dimer, $E_{a,2}$), 89.8 kJ·mol^{-1}, respectively, despite the predominance of the latter amongst the reaction products. This gap in activation energy was corroborated by an Arrhenius plot (Fig. 9) constructed using the initial formation rates of both products calculated with the same experimental dataset used in the integral kinetic study.

The consistency between the numerical and analytical solutions confirms that MLA transesterification to LD has the greater energy barrier of the two alternative pathways. As a result, the preponderance of LD can only be explained by phenomena accounted for by the pre-exponential factor ($k_{0,1}$ and $k_{0,2}$ for ML_2A and LD formation, respectively), such as entropy-related phenomena and active site availability [45]. This is reflected by the larger $k_{0,2}$ value compared to $k_{0,1}$. The model is further validated by the negative enthalpy of adsorption of MLA and methanol (ΔH_{MLA} and ΔH_{MeOH}, respectively) obtained, as adsorption is always exothermic.

These findings indicate that the pathway and mechanism of transesterification of MLA on TiO_2/SiO_2 is accurately approximated by numerical models derived from the analytical mechanistic study outlined above, which imply that: (i) both dimers are directly formed on the catalyst surface from MLA as suggested by the delplot analysis; (ii) two MLA molecules are converted to LD via a rate-limiting Langmuir-Hinshelwood type step as per the initial rate study; (iii) each dimer is formed through a different mechanism as indicated by the initial rate study.

That the numerical solution corroborates the results of the analytical solutions is a good indication of their validity. Because the LHHW rate expression representing an Eley-Rideal type mechanism as rate-determining step better approximated the catalytic performances, it appears that the ambiguous formation of the linear dimer is not determined by the adsorption of MLA which was suggested by the initial rate study, and that neither does it follow a dual-site mechanism, as evidenced by the poor fit of model 3.

3.3.3. Implications of mechanism for alkyl lactate transesterification

Although primarily qualitative, the kinetic model developed provides some insight into the influence of reaction conditions on reaction performances, which has implications for process design. The higher

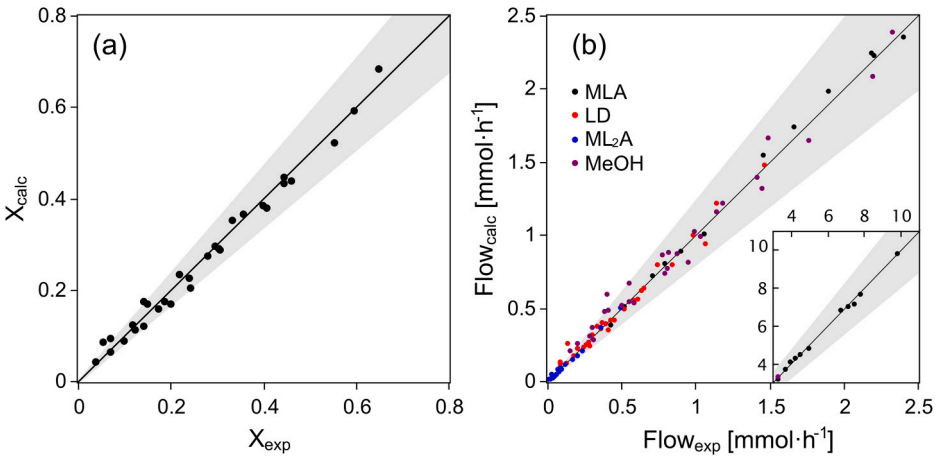

Fig. 8. For the fit of the ER-LH model: (a) Parity plot of the experimental and calculated MLA conversion (black dots); grey area corresponds to ±15% deviation. (b) Parity plot of the experimental and calculated product flows of MLA transesterification; grey area corresponds to ±20% deviation.

Table 2
Kinetic parameters estimated by fitting model ER-LH to experimental data of the transesterification of MLA and their confidence interval.

$\ln(k_{0,1})$	$E_{a,1}$	$\ln(k_{0,2})$	$E_{a,2}$	$K_{0,MLA}$	ΔH_{MLA}	$K_{0,MeOH}$	ΔH_{MeOH}
$mmol \cdot g^{-1} \cdot h^{-1}$	$kJ \cdot mol^{-1}$	$mmol \cdot g^{-1} \cdot h^{-1}$	$kJ \cdot mol^{-1}$	kPa^{-1}	$kJ \cdot mol^{-1}$	kPa^{-1}	$kJ \cdot mol^{-1}$
-3.6 ± 0.0	46.7 ± 1.9	17.7 ± 0.2	89.8 ± 3.6	$(5.0 \pm 0.3)^{-8}$	-47.5 ± 11.9	$(3.8 \pm 0.3)^{-06}$	-29.5 ± 3.1

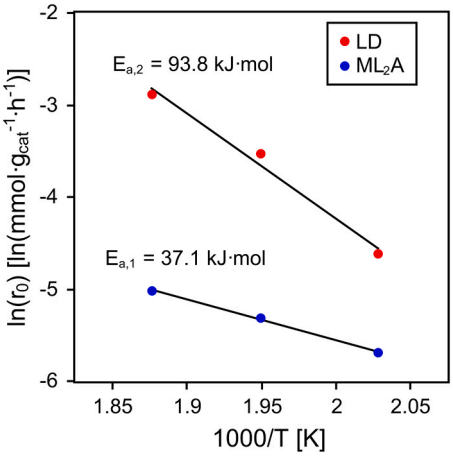

Fig. 9. Arrhenius plots with the apparent activation energy for the formation of LD and ML_2A from MLA (5.9 kPa at atmospheric pressure) with 5 wt% TiO_2/SiO_2 using their initial formation rate.

activation energy of MLA transesterification to LD implies that increasing the temperature will increase cyclization and suppress selectivity towards the linear dimer.

Furthermore, because the inhibiting effect of MLA partial pressure is more pronounced in the formation of LD than it is for methyl lactyl lactate—as expressed in the adsorption term of their respective rate laws—attempts to improve space-time yield by reducing its dilution in the carrier gas will favor the linear dimer formation at the expense of LD. This latter implication may not be detrimental to the process as a whole since alkyl lactyl lactates could be recycled or valorized separately.

If the validity of this mechanism extends to the transesterification of other alkyl lactates, then the implications listed above would also be valid for processes employing other feedstocks. However, a full kinetic study of these other lactates is beyond the scope of this work. Therefore, moving away from integral kinetics, we again employed the initial rate approach, this time using the linearization technique, to quickly assess whether the mechanism deduced for MLA transesterification also applied to other alky lactates.

As mentioned above, when dealing with apparent initial rates, the influence of reversibility and products can be omitted to construct simplified rate law expressions; these laws can be rearranged to express linear relationships between the initial partial pressure of the reactant and the initial rate, and their validity verified by the linearity of the fit to the experimental data [34,46–48].

$$r_{0,app} = \frac{k \cdot K_{lactate}^2 \cdot p_{0,lactate}^2}{(1 + K_{lactate} \cdot p_{0,lactate})^2} \quad (6)$$

$$\frac{p_{0,lactate}}{\sqrt{r_{0,app}}} = \frac{1}{\sqrt{k} \cdot K_{lactate}} + \frac{1}{\sqrt{k}} \cdot p_{0,lactate} \quad (7)$$

Considering that LD is the main product of alkyl lactate transesterification, the mathematical expression of its apparent MLA consumption rate can be approximated to the dual-site mechanism in model ER-LH (Table 1 model 2). Applying the initial rate approximation removes the contribution of methanol to the adsorption term and replaces the effluent lactate partial pressure by its initial value $p_{0,lactate}$ (Eq 6), which affords Eq 7 after linearization.

The plots comparing experimental $p_{0,lactate}/\sqrt{r_0}$ against $p_{0,lactate}$ for MLA, ELA and BLA are illustrated in Fig. 10, (a), (b) and (c), respectively. Fig. 10 (a) demonstrates that the approximations made to the initial rate law of MLA transesterification in Eq 7 are valid, based on the linearity of the plot, but also from the positive abscissa intersect which otherwise would have resulted in invalid negative kinetic parameters. This observation corroborates the validity of the Langmuir-Hinshelwood type mechanism previously deduced through analytical and numerical methods.

Similar linearity can be observed for the plots of ELA and BLA indicating that their apparent transesterification rate can also be expressed by the same rate law (Fig. 10 (b) and (c)), suggesting that alkyl lactate cyclization reactions proceed via the same Langmuir-Hinshelwood mechanism, and that the implications deduced above are also valid irrespective of the alkyl group.

4. Conclusion

In this work, 5 wt% TiO_2/SiO_2 demonstrated that its ability to catalyze the gas-phase transesterification is not limited to MLA, and that other alkyl lactates can successfully be converted to L-LD in high yield. The nature of the ester alkyl chain was shown not to have significant influence on the thermodynamics of the reaction: (i) for all alkyl lactates tested, transesterification reached similar equilibria limitations around 47.5 ± 3.0% conversion, and (ii) product distribution at equilibrium was comparable regardless of the lactate and reaction conditions used, with L-LD being the predominant product. Contrarily, the ester alkyl chain proved to significantly influence the kinetics of alkyl ester transesterification. Using the Taft equation, we determined that the greater the electron donating effect of the alkyl chain, the slower the reaction proceeded, implying that there may exist a point at which the nature of the feedstock would render the reaction impracticable.

A mechanistic study based on MLA provided crucial information about the way alkyl lactate transesterification operates, notably with regards to LD formation. Through analytical methods and a LHHW kinetic study, we demonstrated that LD directly formed from MLA through a Langmuir-Hinshelwood type mechanism and possesse a relatively high activation energy. Other alkyl lactates are likely to follow a similar mechanism, as indicated by an initial rate study which found matching apparent mechanism for ethyl and n-butyl lactate transesterification.

The principal implication of this mechanistic analysis from an industrial point of view is that increasing the reaction temperature will favor LD selectivity, whereas higher alkyl lactate concentration in the carrier gas will be detrimental to it. We foresee that this technology could easily be adapted to suit the availability of alkyl lactate supply, which currently depends on the process used to purify lactic acid [25], to produce L-LD for the manufacturing of high-quality polylactic acid, or other cyclic monomers used in the preparation of bioplastics [28].

CRediT authorship contribution statement

Guillaume Pomalaza: Methodology, Software, Formal Analysis, Writing - Original Draft, Visualization. **Rik De Clercq:** Conceptualization, Methodology, Investigation, Data Curation, Writing - Review & Editing. **Michiel Dusselier:** Conceptualization - Writing - Review & Editing. **Bert Sels:** Conceptualization - Writing - Review & Editing, Supervision, Project administration, Funding acquisition.

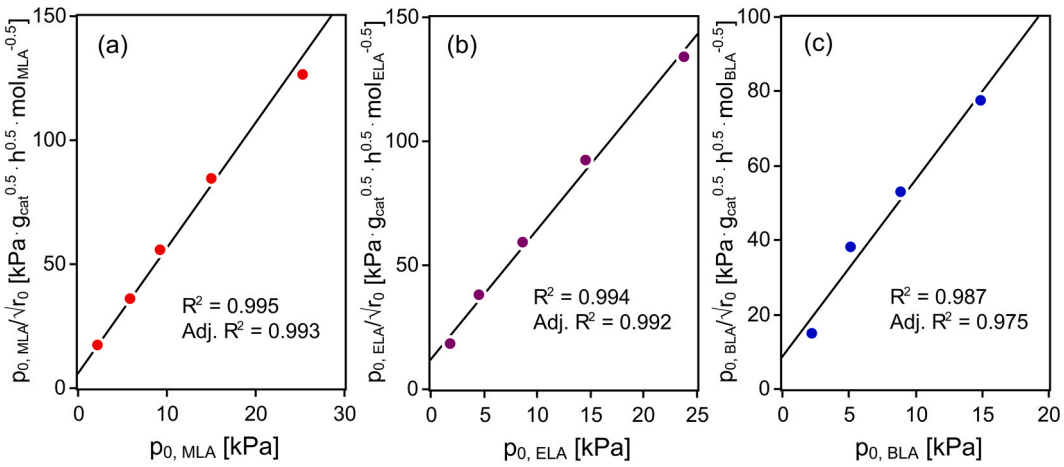

Fig. 10. Plots of $p_0/\sqrt{r_0}$ vs p_0 for the transesterification of (a) MLA, (b) ELA, (c) n-butyl lactate at 220 °C on 5 wt% TiO_2/SiO_2.

Declaration of Competing Interest

The authors declare that they have no known competing financial interests or personal relationships that could have appeared to influence the work reported in this paper.

Acknowledgements

We acknowledge the Agency for Innovation by Science and Technology (IWT, Belgium, project number 131404), the Research Foundation-Flanders (FWO, Belgium, 12E8617N), the Industrial Research Fund (IOF, grant ZKC8139) and the AgriChemWhey project (funded from the Bio-Based Industries Joint Undertaking under the European Union's Horizon 2020 research and innovation program under grant agreement No 744310) for financial support.

Appendix A. Supporting information

Supplementary data associated with this article can be found in the online version at doi:10.1016/j.apcatb.2021.120747.

References

[1] K.G. Harding, J.S. Dennis, H. von Blottnitz, S.T.L. Harrison, Environmental analysis of plastic production processes: comparing petroleum-based polypropylene and polyethylene with biologically-based poly-β-hydroxybutyric acid using life cycle analysis, J. Biotechnol. 130 (1) (2007) 57–66.
[2] A.L. Andrady, Persistence of plastic litter in the oceans. Marine Anthropogenic Litter, Springer,, Cham, 2015, pp. 57–72.
[3] J. Brizga, K. Hubacek, K. Feng, The unintended side effects of bioplastics: carbon, land, and water footprints, One Earth 3 (1) (2020) 45–53.
[4] Market – European Bioplastics e.V. ⟨https://www.european-bioplastics.org/market/⟩ (accessed Jan 15, 2021).
[5] F. Cherubini, The biorefinery concept: using biomass instead of oil for producing energy and chemicals, Energy Convers. Manag 51 (7) (2010) 1412–1421.
[6] H. Kim, S. Lee, Y. Ahn, J. Lee, W. Won, Sustainable production of bioplastics from lignocellulosic biomass: technoeconomic analysis and life-cycle assessment, ACS Sustain. Chem. Eng. 8 (33) (2020) 12419–12429.
[7] P. VanWouwe, M. Dusselier, E. Vanleeuw, B. Sels, Lactide synthesis and chirality control for polylactic acid production, ChemSusChem 9 (9) (2016) 907–921.
[8] H. Cai, V. Dave, R.A. Gross, S.P. McCarthy, Effects of physical aging, crystallinity, and orientation on the enzymatic degradation of poly(Lactic Acid), J. Polym. Sci. B Polym. Phys. 34 (16) (1996) 2701–2708, 270102708.
[9] Global Polylactic Acid Market Size | Industry Report 2020–2027 ⟨https://www.grandviewresearch.com/industry-analysis/polylactic-acid-pla-market⟩ (accessed Dec 21, 2020).
[10] V. Botvin, S. Karaseva, D. Salikova, M. Dusselier, Kinetic study of depolymerization of lactic and glycolic acid oligomers in the presence of oxide catalysts, Polym. (Basel) 12 (2020), 109427.
[11] S. Heo, H.W. Park, J.H. Lee, Y.K. Chang, Design and evaluation of sustainable lactide production process with an one-step gas phase synthesis route, ACS Sustain. Chem. Eng. 7 (6) (2019) 6178–6184.
[12] J. Park, H. Cho, D. Hwang, S. Kim, I. Moon, M. Kim, Design of a novel process for continuous lactide synthesis from lactic acid, Ind. Eng. Chem. Res. 57 (35) (2018) 11955–11962.
[13] T.A. Egiazaryan, V.M. Makarov, M.V. Moskalev, D.A. Razborov, I.L. Fedushkin, Synthesis of lactide from alkyl lactates catalyzed by lanthanide salts, Mendeleev Commun. 29 (6) (2019) 648–650.
[14] H. Tsuji, F. Kondoh, Synthesis of meso-lactide by thermal configurational inversion and depolymerization of poly(L-Lactide) and thermal configurational inversion of lactides, Polym. Degrad. Stab. 141 (2017) 77–83.
[15] Y. Hu, W.A. Daoud, B. Fei, L. Chen, T.H. Kwan, C.S. Ki Lin, Efficient ZnO aqueous nanoparticle catalysed lactide synthesis for poly(Lactic Acid) fibre production from food waste, J. Clean. Prod. 165 (2017) 157–167.
[16] H.W. Park, Y.K. Chang, Economically efficient synthesis of lactide using a solid catalyst, Org. Process Res. Dev. 21 (12) (2017) 1980–1984.
[17] P.P. Upare, J.W. Yoon, D.W. Hwang, U.H. Lee, Y.K. Hwang, D.Y. Hong, J.C. Kim, J. H. Lee, S.K. Kwak, H. Shin, H. Kim, J.S. Chang, Design of a heterogeneous catalytic process for the continuous and direct synthesis of lactide from lactic acid, Green. Chem. 18 (22) (2016) 5978–5983.
[18] V.N. Glotova, M.K. Zamanova, A.V. Yarkova, D.S. Krutas, T.N. Izhenbina, V. T. Novikov, Influence of storage conditions on the stability of lactide, Procedia Chem. 10 (2014) 252–257.
[19] R. De Clercq, M. Dusselier, E. Makshina, B.F. Sels, Catalytic gas-phase production of lactide from renewable alkyl lactates, Angew. Chem. Int. Ed. 57 (12) (2018) 3074–3078.
[20] R. De Clercq, M. Dusselier, C. Poleunis, D.P. Debecker, L. Giebeler, S. Oswald, E. Makshina, B.F. Sels, Titania-silica catalysts for lactide production from renewable alkyl lactates: structure–activity relations, ACS Catal. 8 (9) (2018) 8130–8139.
[21] L. Yang, J. Su, S. Carl, J.G. Lynam, X. Yang, H. Lin, Catalytic conversion of hemicellulosic biomass to lactic acid in PH neutral aqueous phase media, Appl. Catal. B Environ. 162 (2015) 149–157.
[22] K. Nemoto, Y. Hirano, K.I. Hirata, T. Takahashi, H. Tsuneki, K.I. Tominaga, K. Sato, Cooperative In-Sn catalyst system for efficient methyl lactate synthesis from biomass-derived sugars, Appl. Catal. B Environ. 183 (2016) 8–17.
[23] M.N. Simonov, P.A. Zaikin, I.L. Simakova, Highly selective catalytic propylene glycol synthesis from alkyl lactate over copper on silica: performance and mechanism, Appl. Catal. B Environ. 119–120 (2012) 340–347.
[24] P.T. Anastas. Green Chemistry as Applied to Solvents, ACS Publications,, 2002.
[25] C.-Y. Su, C.-C. Yu, I.-L. Chien, J.D. Ward, Plant-wide economic comparison of lactic acid recovery processes by reactive distillation with different alcohols, Ind. Eng. Chem. Res. 52 (32) (2013) 11070–11083.
[26] E.A. Poryvaeva, T.A. Egiazaryan, V.M. Makarov, M.V. Moskalev, D.A. Razborov, I. L. Fedyushkin, Synthesis of lactide from lactic acid and Its esters in the presence of rare-earth compounds, Russ. J. Org. Chem. 53 (3) (2017) 344–350.
[27] V. Brei, A. Varvarin, S. Levytska, Y. Glushchuk, Vapor-phase synthesis of lactide from ethyl lactate over TiO_2/SiO_2 catalyst, Ukr. Chem. J. 85 (7) (2019) 31–37.
[28] R. De Clercq, E. Makshina, B.F. Sels, M. Dusselier, Catalytic gas-phase cyclization of glycolate esters: a novel route toward glycolide-based bioplastics, ChemCatChem 10 (24) (2018) 5649–5655.
[29] C.; Perego, S. Peratello, Experimental methods in catalytic kinetics, Catal. Today 52 (2–3) (1999) 133–145.
[30] P. Virtanen, R. Gommers, T.E. Oliphant, M. Haberland, T. Reddy, D. Cournapeau, E. Burovski, P. Peterson, W. Weckesser, J. Bright, S.J. van der Walt, M. Brett, J. Wilson, K.J. Millman, N. Mayorov, A. Nelson, E. Jones, R. Kern, E. Larson, C. J. Carey, İ. Polat, Y. Feng, E.W. Moore, J. VanderPlas, D. Laxalde, J. Perktold, R. Cimrman, I. Henriksen, E.A. Quintero, C.R. Harris, A.M. Archibald, A.H. Ribeiro, F. Pedregosa, P. van Mulbregt, C. SciPy, SciPy 1.0: fundamental algorithms for scientific computing in python, Nat. Methods 17 (3) (2020) 261–272.
[31] Newville, M.; Stensitzki, T.; Allen, D.B.; Ingargiola, A. LMFIT: Non-Linear Least-Square Minimization and Curve-Fitting for Python. 2014.

[32] M. Schwaab, J.C. Pinto, Optimum reference temperature for reparameterization of the Arrhenius Equation. Part 1: problems involving one kinetic constant, Chem. Eng. Sci. 62 (10) (2007) 2750–2764.
[33] L. Constantinou, R. Gani, New group contribution ethod for estimating properties of pure compounds, AIChE J. 40 (10) (1994) 1697–1710.
[34] E. Santacesaria, R. Tesser. The Chemical Reactor from Laboratory to Industrial Plant, Springer International Publishing: Cham,, 2018.
[35] T.W.G. Solomons, C.B. Fryhle, S.A. Snyder. Solomons' Organic Chemistry, MTM,, 2021.
[36] R.W. Taft, Linear free energy relationships from rates of esterification and hydrolysis of aliphatic and ortho-substituted benzoate esters, J. Am. Chem. Soc. 74 (11) (1952) 2729–2732.
[37] W. Wu, J. Xu, R. Ohnishi, Complete hydrodechlorination of chlorobenzene and its derivatives over supported nickel catalysts under liquid phase conditions, Appl. Catal. B Environ. 60 (1–2) (2005) 129–137.
[38] D. Datta, Taft's substituent constants, Σ* and ΣI, and Huheey's group electronegativity, J. Phys. Org. Chem. 4 (2) (1991) 96–100.
[39] N.A. Bhore, M.T. Klein, K.B. Bischoff, The delplot technique: a new method for reaction pathway analysis, Ind. Eng. Chem. Res. 29 (2) (1990) 313–316.
[40] K.H. Yang, O.A. Hougen, Determination of mechanism of catalyzed gaseous reactions, Chem. Eng. Prog. 46 (3) (1950) 146–157.
[41] J.C. Gee, M.S. Jeansonne, H. Yang, S. Fisher, Reactions of 2-octanol on Amberlyst® 15: concurrent eley–rideal and langmuir–hinshelwood reactions on two different types of active sites, React. Kinet. Mech. Catal. 122 (1) (2017) 21–41.
[42] S. Chaemchuen, P.M. Heynderickx, F. Verpoort, Kinetic modeling of oleic acid esterification with UiO-66: from intrinsic experimental data to kinetics via elementary reaction steps, Chem. Eng. J. 394 (2020), 124816.
[43] T.F. Dossin, M.F. Reyniers, G.B. Marin, Kinetics of heterogeneously MgO-catalyzed transesterification, Appl. Catal. B Environ. 62 (1–2) (2006) 35–45.
[44] E.G. Al-Sakkari, S.T. El-Sheltawy, N.K. Attia, S.R. Mostafa, Kinetic study of soybean oil methanolysis using cement kiln dust as a heterogeneous catalyst for biodiesel production, Appl. Catal. B Environ. 206 (2017) 146–157.
[45] J.K. Nørskov, F. Studt, F. Abild-Pedersen, T. Bligaard. Fundamental Concepts in Heterogeneous Catalysis, John Wiley & Sons, 2014.
[46] T. Takahashi, Kinetics of catalytic disproportionation of propylene, Bull. Jpn. Pet. Inst. 14 (1) (1972) 40–46.
[47] J. Franckaerts, G.F.F. Froment, Kinetic study of the dehydrogenation of ethanol, Chem. Eng. Sci. 19 (10) (1964) 807–818.
[48] X. Van Doorslaer, P.M. Heynderickx, K. Demeestere, K. Debevere, H. Van Langenhove, J. Dewulf, TiO_2 mediated heterogeneous photocatalytic degradation of moxifloxacin: operational variables and scavenger study, Appl. Catal. B Environ. 111–112 (2012) 150–156.